

Available online at www.sciencedirect.com**ScienceDirect**

Energy Procedia 55 (2014) 762 – 768

Energy
Procedia

4th International Conference on Silicon Photovoltaics, SiliconPV 2014

Optical and electronic properties of MAE textured nanoporous silicon

Teck Kong Chong^{a,*}, Klaus Weber^a, Katherine Booker^a, Andrew Blakers^a^a*Australian National University, Research school of Engineering, Canberra, A.C.T. 0200, Australia*

Abstract

We present a 3-step metal-assisted chemical etching (MAE) texturing technique to fabricate nanoporous Si (MAE nSi) using mono- and multi-crystalline silicon (mc-si) substrate. We show that only a very short etch back is necessary to obtain low reflectance. The angular distribution of the reflected light suggests that most of the losses due to the surface reflectance can be recovered after encapsulation and this has been validated in this work. We demonstrate that by using the texturing method shown in this work, very low reflectance can be achieved upon encapsulation. The substantial reduction in reflectance, for some of the textures, upon encapsulation may be partly attributed to the angular distribution of light reflected from the textured surface. Texturing is shown to result in a modest increase in the surface area. However, the increase in the surface recombination rate is smaller than the increase in the surface area, and typically significantly less than a factor of 3, when samples are passivated with atomic layer deposited Al_2O_3 . This result suggests neither the local curvature nor the predominant crystallographic orientation causes additional recombination at the MAE nSi surface. The combination of low surface reflectance and low surface recombination of the MAE nSi makes it a very interesting candidate for solar cell applications.

© 2014 The Authors. Published by Elsevier Ltd. This is an open access article under the CC BY-NC-ND license (<http://creativecommons.org/licenses/by-nc-nd/3.0/>).

Peer-review under responsibility of the scientific committee of the SiliconPV 2014 conference

Keywords: MAE texturing; surface passivations; optics; black silicon; nanoporous silicon

1. Introduction

Surface texturing of silicon (Si) substrates is a well-established technique that has been studied exhaustively. Texturing techniques such as isotexturing and anisotropic random pyramid texturing using acidic and alkaline

* Corresponding author. Tel.: +61 2 61257008; fax: +61 2 612500506.

E-mail address: teck.chong@anu.edu.au

chemical solutions respectively have been widely used by the solar industry to increase solar cell efficiency. These random texturing techniques both reduce surface reflectance and light absorption by ensuring that many light rays undergo total internal reflection (TIR) within the silicon, thus increasing the optical path length of weakly absorbed light. However, neither technique is well suited to the texturing of unconventional substrates produced by technologies such as String Ribbon [1], SiGen [2] or SLIVER [3].

Many other texturing techniques have been investigated either experimentally [4-6] or by simulations [7]. Recently, MAE texturing using Gold (Au) [8-10], Silver (Ag) [11-13] and Palladium (Pd) [14] has been widely studied, and demonstrated to be a flexible and simple process for producing black Silicon (bSi). However, metal contamination (due to the difficulty of removing these noble metals from the silicon surface following texturing) has been reported as a root cause of the observed high surface recombination velocities (S_{eff}) on the bSi [15], likely due to a high interface defect density. The surface area increase as a result of surface texturing has been reported to be another significant cause of high S_{eff} [12].

Surface passivation, in particular by atomic layer deposited (ALD) aluminium-oxide (Al_2O_3) has been shown to provide excellent surface passivation to the bSi [16, 17]. The combination of high negative fixed charge, low defect density of the Al_2O_3 dielectric passivation film at the Si/ Al_2O_3 interface and the conformality of ALD deposited Al_2O_3 film are known to be the key properties that provide such excellent passivation quality for bSi [17-19].

Nevertheless, the understanding of the relationship between optical performance, surface recombination and surface area enhancement is lacking. In this work, we analyse the optical and electronic properties of nSi fabricated with a 3-step Ag nanoparticle-catalysed MAE surface texturing method.

2. Experimental details

2.1 Sample preparation

Low resistivity (1.0-5.0 $\Omega\cdot\text{cm}$) p- and n-type substrates of either (100) or (111) orientation, and p type mc-Si (0.5-2.0 $\Omega\cdot\text{cm}$) were used to fabricate double-sided textured MAE nSi of various morphologies by immersing the Si substrates in aqueous chemical solutions. The thickness of the wafers was 500 μm for the single crystal p type substrates, 300 μm for the n (100) and 250 μm for mc-Si substrates. The wafers were cut into quarters using a dicing saw and then TMAH etched for 15 minutes. This was followed by a brief etch in HF:HNO₃ 1:50 for 1 minute. Any native oxide formed on the surface was removed with 10% HF.

2.2 Texturing

The samples were first immersed in 0.01M AgNO₃:10% HF:H₂O (5:6:98) for 30s to deposit Ag nanoparticles on the surface. Then they were immersed in a solution containing HF:H₂O₂:H₂O (5:3:30) for 3 minutes. Finally the samples, except for one quarter reserved as planar control, were all etched in a solution containing HF:HNO₃:CH₃COOH 1:10:15 for 30s, 60s or 120s. The substrates were rinsed with copious DI water and then blown dry with Nitrogen in between each step. One quarter from each substrate is reserved as a planar control.

2.3 Surface passivation

All MAE nSi samples were passivated with thermal ALD (synthesized in a Beneq TFS-200 ALD system) process was used, using H₂O as the oxidant and trimethyl aluminium (TMAI) as the metal precursor. The thickness of the passivating film was 20nm and the deposition temperature was at 200°C. Prior to the ALD depositions, samples were cleaned in standard RCA solutions to remove any organic and metallic contaminants. Samples were then immersed in a diluted HF solution for a few seconds to remove any native oxide formed on the surface. Following the ALD depositions, samples were annealed in forming gas (FGA) at 400°C for 30 minutes to activate the Al_2O_3 film.

2.4 Characterisation

The optical performance of the bare textured samples was characterized using a UV-Vis spectrophotometer (Perkin-Elmer Lambda 1050) with integrating sphere and Automated Reflectance/Transmittance Analyser (ARTA) module. The minority carrier lifetime was measured using the Sinton quasi steady state photoconductance measurement (QSSPC) technique [20]. Scanning electron microscope (SEM) images were taken using a Zeiss UltraPlus FESEM (field emission scanning electron microscope).

3. Results and discussion

3.1 Optics

Fig. 1 shows cross section and top view SEM images of the etched samples, of the side that was facing up during the etch process ('front side'). The morphology of the back side is very similar to that shown in the corresponding front side images shown here. As can be seen in Fig. 1 below, the variation of the etch back time in HF: HNO₃:CH₃COOH 1:10:15 resulted in different depths of the structure; however, the general surface morphology remained the same regardless of etch back time in the solution. As the etch back time increases, the features become shallower and wider. Eventually the sharp features diminished and a relatively flat surface was obtained. The surface area increases, f_A was estimated to be ranging from ~ 2.5 (longest etch back time) to ~ 3.5 (30s etch back) as compared to an identically prepared planar control.

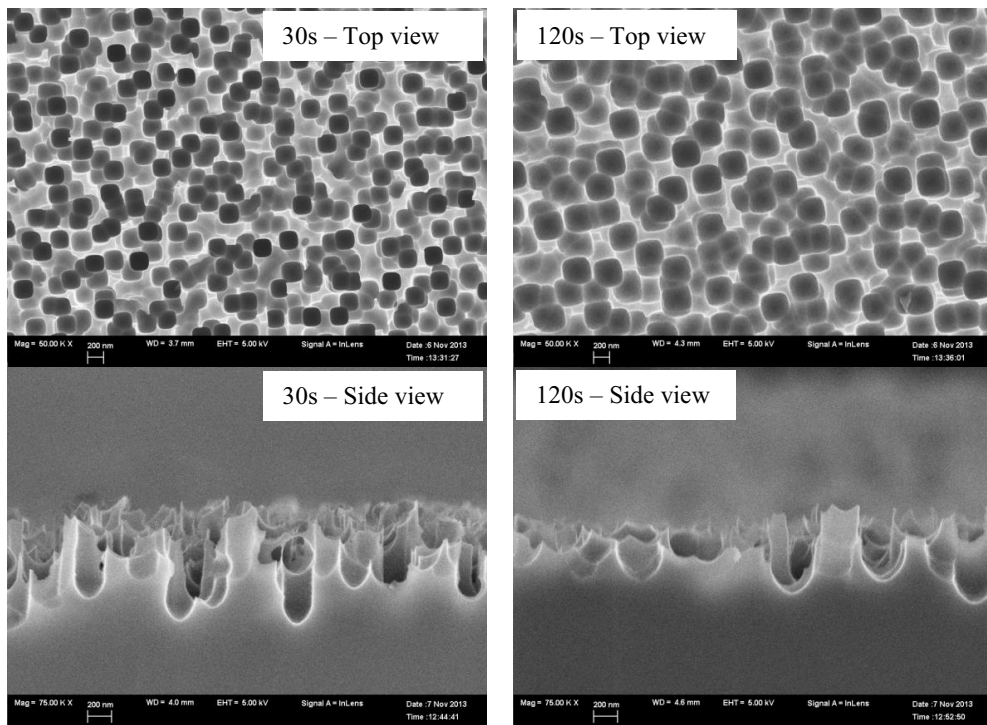


Fig. 1. typical cross-sectional and top SEM views of MAE nSi produced with the 3-step Ag MAE texturing technique. Images on the left have had 30s etch back and images on the right have had 120s etch back in HF:HNO₃:CH₃COOH. Both scale bars are 200nm in length.

It has been shown previously by Stephen et. al that a graded density layer only 200nm thick would be sufficient to make it a very effective absorber [21]. A similar conclusion results from the application of Branz's [8] "scaling law" in which Branz et. al proposed that a nanopore or grade depth of $\sim 250\text{nm}$ can be very efficient in reducing surface reflectance to below 5% out to $\lambda=1000\text{nm}$ [8]. This suggests that the nSi structure resulting from the MAE texturing with etch back times between 30 and 120s should be sufficient to allow surface reflectance on Si to be reduced to less than $\sim 5\%$ throughout the wavelength range λ up to $\sim 1000\text{nm}$. Fig. 2 shows the front surface reflectance measurement of MAE nSi of various etch back time. A planar control sample is also included for comparison.

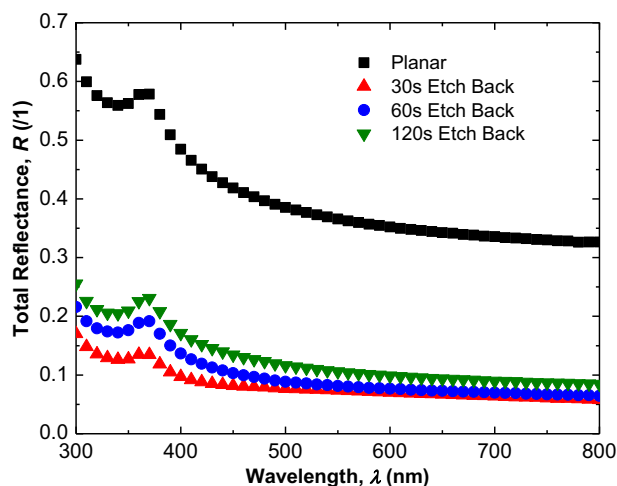


Fig. 2. Total reflectance of bare MAE nSi samples.

It is clear from Fig. 2 that only a very short etch back is necessary to obtain good antireflection performance. It has been observed experimentally that a certain amount of etch back is necessary to reduce porosity on the sample surface in order to reduce surface recombination after the sample is passivated. The etch back step not only serves the purpose of reducing the level of porosity (therefore a slight reduction in the surface area too) on the textured surface, but also removes the Ag particles. This is an important advantage because no additional chemical solution is required to remove the remaining particles. The additional step to remove metallic particles [13, 22] can be complicated and inefficient [15] perhaps due to the problem with wettability of the sample surfaces. Nonetheless, the benefit of reducing porosity and metallic particle (Ag) in one step comes at the cost of a slightly higher surface reflectance compared to that of bSi [10, 15, 23] or the sample without any etch back in our experiment. The total surface reflectance (R) of samples with 30s and 60s etch back is similar. As the etch back time increases to 120s, the reflectance curve shifts upwards. At long wavelengths ($\lambda > 1000\text{nm}$), R increases dramatically due to light reflected from the textured back surface and reaching the front surface without being absorbed. Although not shown here, the textured mc-Si samples gave very similar results. Hence the texturing technique can be applied equally well to mc-Si.

Fig. 3 shows the angular distribution of reflected light of MAE nSi, where all the curves were scaled to have a peak of 1.

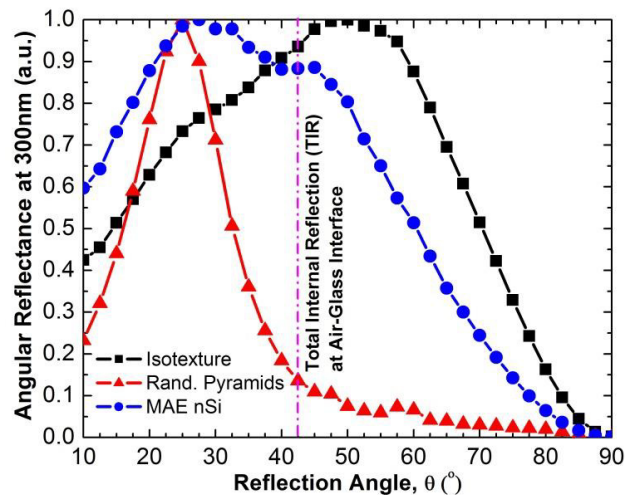


Fig. 3. Comparison of normalized angular distribution reflectance. MAE nSi samples of 60s etch back was used. A random pyramidal and isotexture sample was also included for comparison

The fraction of light reflected at $>42^\circ$ (which will result in total internal reflection at the glass-air interface) from the MAE nSi surface is smaller than for the isotexture sample but significantly better than for the random pyramid structure. Given the lower reflectance of MAE nSi compared to isotexture, these measurements suggest that the encapsulated reflectance of the MAE nSi samples will be superior to that of both the random pyramid and isotexture samples.

Following the optical measurement of MAE nSi discussed above, the same MAE nSi structures were encapsulated (both sides) with silicone (SLM TPSE 177 PV film from Tectosil, $\sim 200\mu\text{m}$ on each side) and a cover sheet (Tefzel® Fluoropolymer Film, $\sim 50\mu\text{m}$). The surface reflectance measurement of the encapsulated samples is plotted in Fig. 4 below. Reflectance from bare samples is also included for comparison.

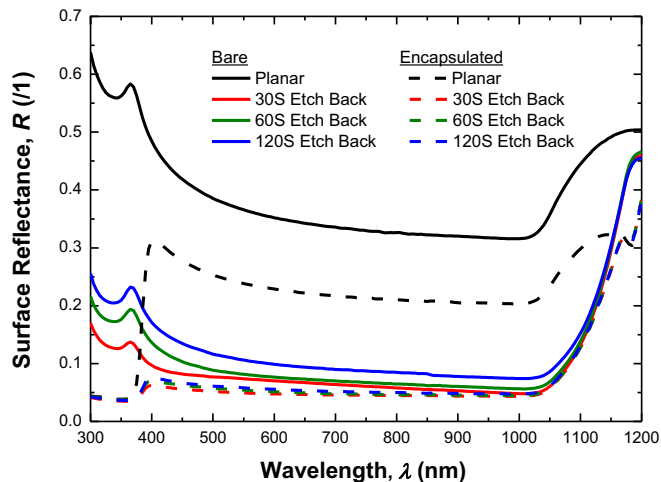


Fig. 4. Comparison of the front surface reflectance of bare and encapsulated MAE nSi samples.

As can be seen from Fig. 4, all samples have significantly reduced front surface reflectance in comparison to the samples without encapsulation. Only small differences in surface reflectance are observed between the various etch back samples after encapsulation. The apparent reduction in surface reflectance below 400nm is due to absorption in the encapsulant. The low reflectance values demonstrate the excellent optical performance of the MAE nSi texture under encapsulation, without the presence of an AR coating. The reflectance curves include the ~3% reflectance at the encapsulant/air interface, which means the additional reflectance due to the Si sample is less than 2% for the best sample (30s etch back) and for $\lambda > 600\text{nm}$.

3.2 Surface passivation

The effective minority carrier lifetime of all samples was measured using the transient photoconductance decay method [20] at a carrier injection level $\Delta n = 10^{15}\text{cm}^{-3}$. S_{eff} was calculated using the well-known relationship (valid for low S_{eff}):

$$S_{eff} = \left[\frac{1}{\tau_{eff}} - \frac{1}{\tau_{bulk}} \right] \left[\frac{w}{2} \right] \quad (1)$$

where τ_{eff} is the measured minority carrier lifetime, w is the substrate thickness and the upper limit of the effective surface recombination S_{eff_UL} was calculated by assuming τ_{bulk} is limited by Auger and radiative recombination only, and employing the parameterisation of Richter et al.[24]. The same assumption is also applied to calculate the S_{eff_UL} for mc-Si samples.

Fig. 5 below shows the S_{eff_UL} value of planar control and samples of various etch back time.

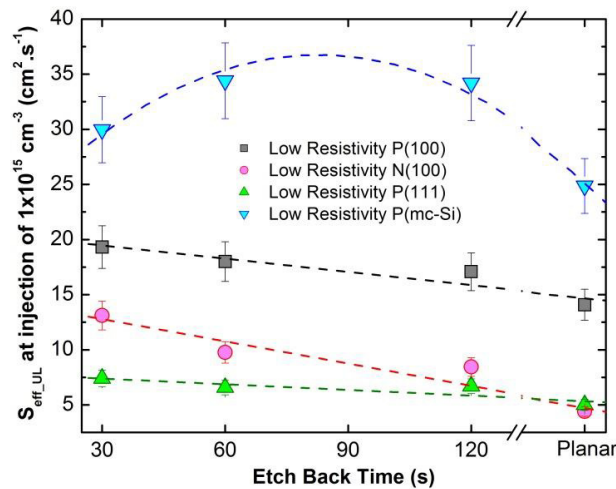


Fig. 5. Effective maximum surface recombination velocity (S_{eff_UL}) as a function of etch back time. Note that 10% of error is anticipated.

As shown in Fig 5, all MAE nSi textures (using mono-crystalline silicon substrates) exhibit S_{eff_UL} values below 20 cm.s^{-1} , with the value decreasing with increasing etch back time. Higher S_{eff} at undiffused mc-Si substrate is expected since mc-Si is known to have much higher defects such as grain boundary and dangling bonds. However, the increase of S_{eff} on the textured mc-si samples are not linearly dependent on the surface area increase f_A . Despite the nonlinear relationship, about a factor of 2 increases in S_{eff} for the textured samples as compared to the p-type mono counterpart is likely due to the variation of bulk lifetime of the samples (bulk limited). Nevertheless, these

results suggest that neither the presence of sharp edges and corners, nor the predominant crystallographic orientation cause additional recombination at the MAE nSi surface.

4. Conclusions

We demonstrated that MAE nSi displays excellent optical properties, in terms of reduced reflectance of both bare and encapsulated samples. The surface reflectance can be reduced significantly at all wavelengths even by relatively shallow etches with small aspect ratios and surface areas. Angular distribution reflectance measurements suggest that a significant fraction (~40%) of the reflected light will have a second chance to be absorbed following encapsulation, which is supported by the reflectance measurements. The coating of MAE nSi samples with thermal ALD deposited Al_2O_3 films allow excellent surface passivation to be realised for a large range of low resistivity substrates and different crystallographic orientations. Further, measurements show that the increase in surface recombination following texturing is no larger than the increase in surface area as a result of texturing. Higher $S_{\text{eff_UL}}$ found on mc-Si samples as compared to mono-crystalline Si samples is likely due to the overestimated τ_{bulk} following the assumption made in this case; as a result no definitive conclusion can be drawn. Nevertheless, the results show that ALD Al_2O_3 is able to provide excellent passivation on all different crystal orientations as well as the sharp peaks, edges and valleys present on the surfaces. Given the low surface area increase required for excellent optical performance, the results suggest that both optical and electronic performance can be optimised without substantial trade-offs between the two.

Acknowledgements

The author (TK) is grateful for the award of APA(I) scholarship. We would like to thank Jonathan Wilson and Martin Berry for encapsulating the samples and the Centre for Advanced Microscopy (CAM) at ANU for SEM access. This project was partly funded by the Australian Research Council through the Linkage grants scheme, project LP100100741.

References

- [1] Hahn, G., Schönecker, A., J Phys: Cond Matt. 2004, 16, R1615.
- [2] Henley, F., Lamm, A., Kang, S., Liu, Z., Tian, L., Proc. 23rd PVSEC. Valencia Spain 2008, 1090-1093.
- [3] Weber, K., Blakers, A., Stocks, M., Babaei, J., et al., Elect Dev Lett, IEEE. 2004, 25, 37-39.
- [4] Winderbaum, S., Reinhold, O., Yun, F., Sol energ mat sol c. 1997, 46, 239-248.
- [5] Wu, C., Crouch, C., Zhao, L., Carey, J., et al., Appl Phys Lett. 2001, 78, 1850-1852.
- [6] Zhu, J., Hsu, C. M., Yu, Z., Fan, S., Cui, Y., Nano Lett. 2009, 10, 1979-1984.
- [7] Chong, T. K., Wilson, J., Mokkaapati, S., Catchpole, K. R., J Opt. 2012, 14, 024012.
- [8] Branz, H. M., Yost, V. E., Ward, S., Jones, K. M., et al., Appl Phys Lett. 2009, 94, 231121.
- [9] Koynov, S., Brandt, M. S., Stutzmann, M., Appl Phys Lett. 2006, 88, 203107-203107-203103.
- [10] Yuan, H.-C., Yost, V. E., Page, M. R., Stradins, P., et al., Appl Phys Lett. 2009, 95, 123501-123501-123503.
- [11] Nishioka, K., Sueto, T., Saito, N., Appl Surf Sci. 2009, 255, 9504-9507.
- [12] Srivastava, S. K., Kumar, D., Sharma, M., Kumar, R., Singh, P., Sol energ mat sol c. 2012, 100, 33-38.
- [13] Oh, J., Yuan, H. C., Branz, H. M., Nat nano. 2012, 7, 743-748.
- [14] T.K. Chong, K. J. W., Andrew W. Blakers, Proc. 39th IEEE Photo Special Conf. Tampa Florida USA 2013.
- [15] Shi, J., Xu, F., Ma, Z., Zhou, P., et al., Mat Sci Semi Proc. 2013, 16, 441-448.
- [16] Repo, P., Haarahiltunen, A., Sainiemi, L., Yli-Koski, M., et al., IEEE J Photo. 2013, 3, 90-94.
- [17] Otto, M., Kroll, M., Kasebier, T., Salzer, R., et al., Appl Phys Lett. 2012, 100, 191603-191603-191604.
- [18] Repo, P., Benick, J., Gastrow, G. v., Vähäniemi, V., et al., phys stat sol (RRL). 2013, 7, 950-954.
- [19] Wang, W.-C., Lin, C.-W., Chen, H.-J., Chang, C.-W., et al., ACS appl mat & inter. 2013, 5, 9752-9759.
- [20] Sinton, R. A., Cuevas, A., Appl Phys Lett. 1996, 69, 2510-2512.
- [21] Stephens, R. B., Cody, G. D., Thin sol fil. 1977, 45, 19-29.
- [22] Algasinger, M., Paye, J., Werner, F., Schmidt, J., et al., Adv Energy Mat. 2013, 3, 1068-1074.
- [23] Repo, P., Benick, J., Vähäniemi, V., Schön, J., et al., Energ Proc. 2013, 38, 866-871.
- [24] Richter, A., Glunz, S. W., Werner, F., Schmidt, J., Cuevas, A., Phys RevB. 2012, 86, 165202.